Proceedings Paper:
Bakhit, M., Khattak, F.A. orcid.org/0000-0003-2401-9366, Schlecht, S.J. et al. (2 more authors) (Accepted: 2025) Challenges to Subcarrier MIMO Precoding and Equalisation with Smooth Phase Responses. In: Proceedings of 28th International Workshop on Smart Antennas 2025. 2025 28th International Workshop on Smart Antennas (WSA), 16-18 Sep 2025, Erlangen, Germany. IEEE (In Press)

Challenges to Subcarrier MIMO Precoding and Equalisation with Smooth Phase Responses

M.A. Bakhit[1], F.A. Khattak[2], S.J. Schlecht[3], G.W. Rice[4], and S. Weiss[1]
[1]Department of Electronic and Electrical Engineering, University of Strathclyde, Glasgow, Scotland
[2]School of Computer Science, University of Leeds, Leeds LS2 9JT, UK
[3]Multimedia Communications and Signal Processing, Friedrich-Alexander Universität Erlangen-Nürnberg, Germany
[4]Mathworks Ltd., Glasgow, Scotland
{mohammed.bakhit,stephan.weiss}@strath.ac.uk, f.a.khattak@leeds.ac.uk, sebastian.schlecht@fau.de, grice@mathworks.com

***Abstract*—Precoding for multiple-input multiple-output orthogonal frequency division multiplexing systems is often based on a per-subcarrier singular value decomposition, where phase smoothing is applied to the singular vectors that form the transmit beamformers. We show that such a smooth solution can ideally be based on an analytic singular value decomposition, but for estimated channel matrices is beset by challenges that deny a smooth or even continuous evolution of singular vectors with frequency. We show how such problems can be bypassed by admitting complex-valued singular values or fractional delays, and by exploiting a method analogous to the analytic eigenvalue decomposition to approximate ground truth analytic singular vectors from estimated channel matrices. We present examples and demonstrate some of the capabilities of a proposed algorithm through simulations.**

I. Introduction

For the transmission over a multiple-input multiple-output (MIMO) channel, in the narrowband case a singular value decomposition (SVD, [1], [2]) of the channel matrix can provide precoding and equalisation — also referred to more generally as transmit- and receive-beamforming — via its left- and right-singular vectors; such an arrangement satisfies optimality in various senses [3], [4]. For broadband systems, every pair of transmit and receive antennas is described by an impulse response; thus the channel matrix $\mathbf{C}[n]$ now depends on the discrete time index $n \in \mathbb{Z}$. In the z-domain, $\boldsymbol{C}(z) = \sum_n \mathbf{C}[n]z^{-n}$ is a matrix of channel transfer functions, which instead of the narrowband case of a standard matrix with complex valued elements now contains functions in $z \in \mathbb{C}$. Applying the SVD to $\mathbf{C}[n]$ or $\boldsymbol{C}(z)$ is generally only capable of decoupling such a system for a particular value of n or z [5].

To extend this utility of the SVD to broadband systems, an SVD can be applied in every subcarrier of an orthogonal frequency division multiplexing (OFDM) system, see e.g. [6]. A non-uniqueness for the phase of the left- and right-singular vectors in the per-subcarrier SVD can lead to leakage effects [7], and poses challenges for some additional processing tasks such as channel estimation [8]–[10]. In order to achieve some form of smoothness across subcarriers, suggested solutions include methods such as clustering [11], [12], spherical interpolation [11], or geodesical interpolation [13]. In clustering [11] a number of adjacent subcarriers are grouped together and receive a common transmit beamformer, which can be optimised based on maximising the minimum channel gain under a spherical constraint to maintain the unit norm of a singular vector [11]. Alternative, the optimisation can include a smoothness term applied to the channel frequency response, which due to the time-bandwidth product of the Fourier transform and the channel assumed to being shorter than the cyclic prefix on the presumed support of the channel being shorter than the cyclic prefix cannot vary wildly [12], [14]. The latter has also been applied without clustering [7], [15]. The geodesic interpolation in [13] finds the shortest connection between singular vectors in adjacent bins that satisfy mutual orthogonality.

In this paper, we want to explore such OFDM-MIMO techniques against the background of findings from polynomial matrix algebra [5], [16], [17], and explore some of the resulting challenges that appear to not have been addressed in e.g. [7], [9]–[15]. For a channel matrix $\boldsymbol{C}(z)$ that is analytic in z, except for contrived cases there exists an analytic singular value decomposition for $\boldsymbol{C}(z)$ [18]–[20],

$$\boldsymbol{C}(z^{\kappa}) = \boldsymbol{U}(z)\boldsymbol{\Sigma}(z)\boldsymbol{V}^{\mathrm{P}}(z) \; , \qquad (1)$$

with analytic paraunitary factors $\boldsymbol{U}(z)$ and $\boldsymbol{V}(z)$, and an analytic diagonal matrix $\boldsymbol{\Sigma}(z)$. Generally we have $\kappa = 1$ but in some cases require $\kappa = 2$ to admit analytic factors such that $\boldsymbol{\Sigma}(z)$ is a parahermitian matrix, i.e. $\boldsymbol{\Sigma}^{\mathrm{P}}(z) := \{\boldsymbol{\Sigma}(1/z^*)\}^{\mathrm{H}} = \boldsymbol{\Sigma}(z)$ and thus is real-valued on the unit circle. The parahermitian operator $\{\cdot\}^{\mathrm{P}}$ implies time reversal and Hermitian transposition, while paraunitarity means that $\boldsymbol{U}(z)\boldsymbol{U}^{\mathrm{P}}(z) = \mathbf{I}$ [21]. Interestingly, and akin to the case of continuous-time analytic SVD [22], [23], the singular values may have to be permitted to change sign in order to admit the factors in (1) to be analytic.

In principle, analyticity of the SVD factors in (1) implies infinite differentiability of the left- and right-singular vectors, and therefore provides (i) the theoretical foundation for the phase smoothness considerations in [7], [11]–[15], [24], [25], and (ii) implies a potentially stronger smoothness criterion, such that analyticity can be directly exploited to drive algorithms for extracting both analytic eigenvectors [26], [27]

M.A. Bakhit is funded by Mathworks Ltd and the University of Strathclyde.

and analytic singular vectors [28]–[31], and therefore any precoding matrices. However, two facts in this context impact on the application of MIMO precoding:

(F1) in the case $\kappa = 2$, singular values are only 4π periodic, and no analytic solution exists unless either (i) the channel matrix is oversampled [18], [19] or (ii) singular values are permitted to be complex valued [20] on the unit circle;

(F2) if estimated from data, the channel matrix $\boldsymbol{C}(z)$ is randomly perturbed and the singular values and singular vectors of this estimated matrix are only piece-wise analytic [29].

Thus, in such cases no smooth decomposition exists for an estimated channel matrix, contradicting the assumptions made in [7], [11]–[15], [24], [32]. This similarly affects wideband precoding and equalisation as e.g. attempted in [33]–[36], which is based on a polynomial SVD from [16] and may only represent a piecewise analytic approximation of an analytic SVD [19].

In the following, we outline the above facts (F1) and (F2), and demonstrate how an analytic solution can be found using fractional delays [37] and an approximation of the analytic ground truth [38] underlying the estimated channel matrix. The Matlab implementations to generate all figures presented in this paper can be found online[1].

II. MIMO Channel Model

A. MIMO System Transfer Function

For a MIMO broadband system with M transmitters and L receivers, an impulse response $c_{\ell,m}[n]$ can be measured between the mth transmitter and the ℓth receiver. If $c_{\ell,m}[n]$ is causal and stable, the z-transform $C_{\ell,m}(z) = \sum_n c_{\ell,m}[n] z^{-n}$, or for short $C_{\ell,m}(z) \bullet\!\!-\!\!\circ\, c_{\ell,m}[n]$, will be analytic in $z \in \mathbb{C}$. With $\mathbf{C}[n]$ an $L \times M$ matrix of impulse responses with $c_{\ell,m}[n]$ forming its entry in the ℓth row and mth column, $\boldsymbol{C}(z) \bullet\!\!-\!\!\circ\, \mathbf{C}[n]$ is a matrix of analytic functions.

For simplicity, but without loss of generality, in the remainder of the paper we assume $M = L$. We also assume that $\boldsymbol{C}(z)$ has full spatial rank, i.e. that when evaluated on the unit circle, $z = \mathrm{e}^{\mathrm{j}\Omega}$, the determinant $\det\{\boldsymbol{C}(\mathrm{e}^{\mathrm{j}\Omega})\}$ only possesses isolated zero-crossings at most [31], and that we can find at least one Ω_0, where $\boldsymbol{C}(\mathrm{e}^{\mathrm{j}\Omega_0})$ possesses M distinct singular values.

B. Per-Subcarrier Singular Value Decomposition

In an OFDM transmission with K subcarriers, SVD-based decoupling of the channel matrix can yield precoders and equalisers that are optimal in various senses [4]. For this, an SVD is applied to each of the K frequency bins $\boldsymbol{C}(\mathrm{e}^{\mathrm{j}\Omega_k})$, $\Omega_k = 2\pi k/K$, $k = 0, \ldots, (K-1)$,

$$\boldsymbol{C}(\mathrm{e}^{\mathrm{j}\Omega_k}) = \mathbf{U}_k \boldsymbol{\Sigma}_k \mathbf{V}_k^{\mathrm{H}} = \sum_m \sigma_{k,m} \mathbf{u}_{k,m} \mathbf{v}_{k,m}^{\mathrm{H}} \; , \qquad (2)$$

[1] https://github.com/StephanWeiss5/WSA25-precoding

where the diagonal matrix $\boldsymbol{\Sigma}_k$ holds the singular values $\sigma_{k,m}$, and the corresponding left- and right-singular vectors $\mathbf{u}_{k,m}$ and $\mathbf{v}_{k,m}$ form the columns of the unitary matrices $\mathbf{U}_k$ and $\mathbf{V}_k$.

For the sake of uniqueness, the singular values are positive real and ordered such that $\sigma_{k,m} \geq \sigma_{k,m+1} \geq 0$ for $m = 1, \ldots, (M-1)$. However, even with distinct singular values, their corresponding singular vectors possess a phase ambiguity, such that with an arbitrary phase φ_k, $\mathbf{u}_k \mathrm{e}^{\mathrm{j}\varphi_k}$ and $\mathbf{v}_k \mathrm{e}^{\mathrm{j}\varphi_k}$ are also valid left- and right-singular vectors of $\boldsymbol{C}(\mathrm{e}^{\mathrm{j}\Omega_k})$. It is this ambiguity that the MIMO-OFDM schemes in e.g. [7], [11]–[15], [24], [25], [32] aim to resolve, in order to obtain a smooth variation of the singular vectors across frequency bins.

C. OFDM Interpolated Precoding and Equalisation

In MIMO-OFDM systems, the MIMO channel is typically identified in a limited number $K_0 \ll K$ of so-called pilot subcarriers, and the channel gains in the remaining subcarriers are determined by interpolation. If the indices of the pilot subcarriers belong to a set $\mathcal{S}_0$ with cardinality $|\mathcal{S}_0| = K_0$, then the problem is to determine the remaining $K - K_0$ precoders and equalisers via (2). This assumes that the factors in (2) permit an interpolation, i.e. that the r.h.s. of (2) is sampled from sufficiently smooth functions. We show below that this assumption cannot necessarily be made, and that issues arise for the precoding approaches in [7], [11]–[15], [24], [25], [32] when singular values are

(i) constrained to be strictly non-negative,
(ii) constrained to be real-valued, and
(iii) obtained from an estimated channel matrix that is subject to random estimation errors.

In order to demonstrate this, we first explore the theoretical foundations of a frequency-dependent analytic SVD in Sec. III, and some fundamental and profound effects of its perturbation in Sec. IV. A potential solution is highlighted in Sec.V.

III. Analytic Singular Value Decomposition

A. Existence of an Analytic SVD

For the analytic MIMO transfer function matrix $\boldsymbol{C}(z)$, except for contrived cases, an analytic singular value decomposition exists, such that [18], [19]

$$\boldsymbol{C}(z^{\kappa}) = \boldsymbol{U}(z)\boldsymbol{\Sigma}(z)\boldsymbol{V}^{\mathrm{P}}(z) \; . \qquad (3)$$

In (3), $\boldsymbol{U}(z)$ and $\boldsymbol{V}(z)$ are paraunitary matrices, such that e.g. $\{\boldsymbol{U}(z)\}^{-1} = \boldsymbol{U}^{\mathrm{P}}(z)$. The diagonal matrix $\boldsymbol{\Sigma}(z)$ contains the singular values. These can be selected to be real-valued on the unit circle, but must be permitted to change sign akin to the case of the analytic SVD on a real interval [22], [23].

Since analytic singular values may intersect, the majorisation of singular values in the standard SVD [2] does no longer have the same meaning, and their ordering can be arbitrary; they a sign ambiguity [37]. For distinct singular values in $\boldsymbol{\Sigma}(z)$, each corresponding pair of left- and right-singular vectors is non-unique w.r.t. an arbitrarily selected

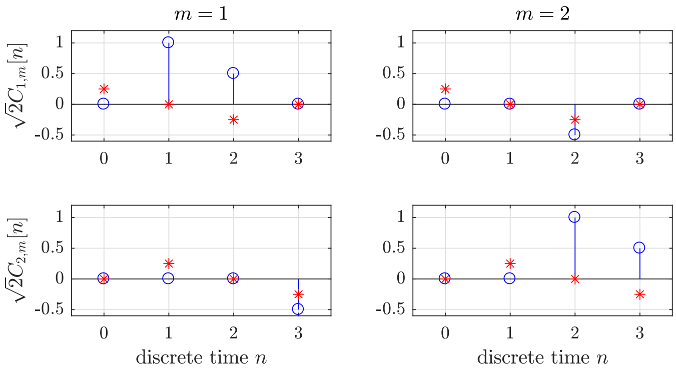

Fig. 1. Elements $C_{\ell,m}[n]$ of matrix $\mathbf{C}[n]$ of Example 1, showing real ($\circ$) and imaginary parts ($*$).

allpass filter [19]. Generally in (3), we have $\kappa = 1$, but if the singular values are constrained to be real on the unit circle and posses an odd number of zero crossings on a 2π interval, $\kappa = 2$ is required in order for (3) to admit r.h.s. factors that are analytic in $z \in \mathbb{C}$, i.e. an analytic SVD with $\boldsymbol{\Sigma}(\mathrm{e}^{\mathrm{j}\Omega}) \in \mathbb{R}^{M\times M}$ only exists for a twice oversampled channel matrix $\boldsymbol{C}(z^2)$.

Example 1: Consider the 2×2 matrix $\boldsymbol{C}(z)$ •—○ $\mathbf{C}[n]$ of analytic functions characterised in Fig. 1. A factorisation can yield

$$\boldsymbol{U}(z) = \frac{z^{-1}}{\sqrt{2}}\begin{bmatrix} 1 & 1 \\ z^{-1} & -z^{-1}\end{bmatrix}, \quad \boldsymbol{V}(z) = \frac{1}{\sqrt{2}}\begin{bmatrix} 1 & z^{\frac{1}{2}} \\ 1 & -z^{\frac{1}{2}}\end{bmatrix}$$

and

$$\boldsymbol{\Sigma}(z) = \begin{bmatrix} \frac{\mathrm{j}}{2}z + 1 - \frac{\mathrm{j}}{2}z^{-1} & 0 \\ 0 & z^{\frac{1}{2}} + z^{-\frac{1}{2}}\end{bmatrix} . \quad (4)$$

With $\boldsymbol{\Sigma}(z) = \mathrm{diag}\{\sigma_1(z), \sigma_2(z)\} = \boldsymbol{\Sigma}^{\mathrm{P}}(z)$ satisfying parahermitian symmetry, its singular values are real-valued on the unit circle. While $\sigma_1(z)$ and its corresponding singular vectors are analytic, and $\sigma_1(\mathrm{e}^{\mathrm{j}\Omega}) \geq 0$, the second singular value exhibits two oddities:

1) $\sigma_2'(\Omega) = \sigma_2(z)|_{z=\mathrm{e}^{\mathrm{j}\Omega}}$ must be permitted to change sign, as otherwise it becomes non-differentiable at $\Omega = (2k+1)\pi$, $k \in \mathbb{Z}$, as evident from Fig 2;
2) $\sigma_2(z)$ contains fractional powers of z and is therefore not analytic; equivalently, its evaluation on the unit circle, $\sigma_2'(\Omega)$ is only 4π-periodic as shown in Fig. 2.

Note that the singular value $\sigma_2'(\Omega)$ only has an odd number of zero crossings over a 2π interval, thus requiring oversampling by $\kappa = 2$. △

Thus, Example 1 demonstrates a case where no analytic SVD with real singular values exists unless the channel is oversampled by a factor of two. Even if oversampled, singular values have to be permitted to change sign in order to admit analytic and hence smooth singular vectors. Therefore, in this case the efforts in [7], [11]–[15], [24], [32] will fail to find a smooth solution.

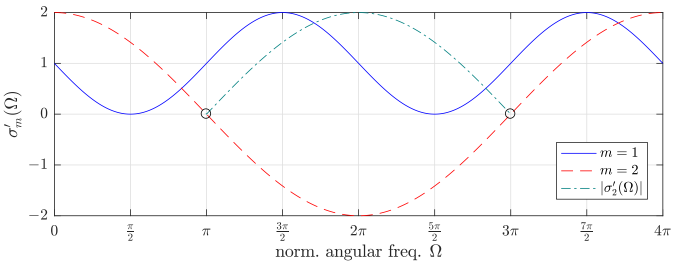

Fig. 2. Singular values of $\boldsymbol{C}(z)$ of Example 1 evaluated on the unit circle.

B. Admitting Complex-Valued Singular Values

As an alternative to (3), admitting complex-valued singular values on the unit circle removes the need for oversampling [20], [37],

$$\boldsymbol{C}(z) = \boldsymbol{U}(z)\boldsymbol{S}(z)\boldsymbol{V}^{\mathrm{P}}(z) , \quad (5)$$

whereby $\boldsymbol{S}(\mathrm{e}^{\mathrm{j}\Omega})$ is diagonal but no longer constrained to be real-valued. This introduces additional ambiguities, and it is now possible to shift allpass factors between singular values and singular vectors.

Example 2: For the matrix $\boldsymbol{C}(z)$ of Example 1 it is possible to find a complex-valued analytic SVD with

$$\boldsymbol{U}(z) = \frac{z^{-1}}{\sqrt{2}}\begin{bmatrix} 1 & 1 \\ z^{-1} & -z^{-1}\end{bmatrix}, \quad \boldsymbol{V}(z) = \frac{1}{\sqrt{2}}\begin{bmatrix} 1 & 1 \\ 1 & -1\end{bmatrix}$$

and

$$\boldsymbol{S}(z) = \begin{bmatrix} \frac{\mathrm{j}}{2}z + 1 - \frac{\mathrm{j}}{2}z^{-1} & 0 \\ 0 & 1 + z^{-1}\end{bmatrix} . \quad (6)$$

In contrast to the analytic SVD with real-valued singular values in Example 1, all factors are now analytic, as the fractional delay $z^{-\frac{1}{2}}$ — an ideal allpass — has been shifted between the second singular value and its corresponding right-singular vector. △

IV. Analytic SVD Under Random Perturbation

A. Channel Matrix Estimation

If a MIMO channel $\boldsymbol{C}(z)$ is estimated, then the estimate $\hat{\boldsymbol{C}}(z)$,

$$\hat{\boldsymbol{C}}(z) = \boldsymbol{C}(z) + \boldsymbol{E}(z) , \quad (7)$$

is subject to a random perturbation term $\boldsymbol{E}(z)$. This may occur e.g. when a channel is identified by an adaptive system identification setup [39], [40], or if a channel is sounded using finite data — say N samples — or under the influence of channel noise. Typically the size of this perturbation term will depend on the sample size N on which the estimate is based, as well as the exact channel and the signal statistics [41], [42]. The larger the sample size N is, the smaller the perturbation term becomes.

We know that for an analytic perturbation of $\boldsymbol{C}(z)$, the perturbation of the analytic SVD factors will also be analytic [18], [19]. Thus, a small change in $\boldsymbol{C}(z)$ will only result in a small variation in its analytic SVD factors [43]. For a

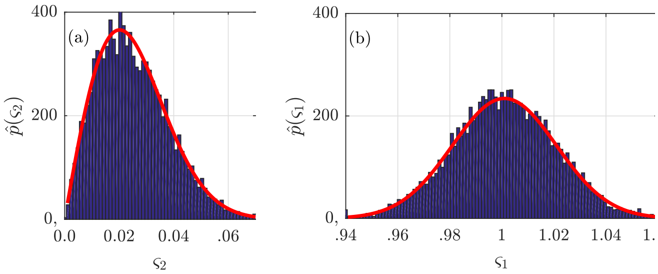

Fig. 3. Histograms of bin-wise singular values ς_m, $m = 1, 2$, at $\Omega = \pi$; t
fitted curves are Rician distributions.

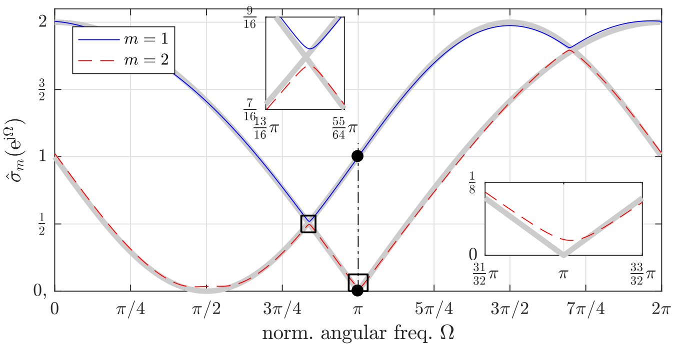

Fig. 4. Analytic singular values of $\hat{\boldsymbol{C}}(z)$ on the unit circle, with the moduli of the analytic singular values of $\boldsymbol{C}(z)$ underlaid in grey. The vertical line at $\Omega = \pi$ indicates where the histograms of Fig. 3 are evaluated.

random perturbation this is not guaranteed to be true, and a small random perturbation of $\boldsymbol{C}(z)$ could potentially result in a significant perturbation of its analytic SVD factors. We will explore this below.

B. Perturbation of Singular Values

On a bin-wise perspective, the random perturbation by $\boldsymbol{E}(\mathrm{e}^{\mathrm{j}\Omega})$ causes the singular values to become random variables with a distribution. Two fundamental effects occur. Firstly, if $\boldsymbol{A}(\mathrm{e}^{\mathrm{j}\Omega_0})$ for some frequency Ω_0 possesses two identical eigenvalues, then by sampling from a distribution, almost surely the singular values of $\hat{\boldsymbol{A}}(\mathrm{e}^{\mathrm{j}\Omega_0})$ will be distinct [44]. Secondly, if a singular value of $\boldsymbol{A}(\mathrm{e}^{\mathrm{j}\Omega_0})$ was zero, then the singular value of $\hat{\boldsymbol{A}}(\mathrm{e}^{\mathrm{j}\Omega_0})$ will have a positive offset term [43].

Example 3: We perturb the earlier system $\boldsymbol{C}(z)$ of Example 1 by 10^4 uncorrelated complex Gaussian instances $\boldsymbol{E}(z)$ of the same support as $\boldsymbol{C}(z)$ at a signal-to-noise ratio (SNR) of 40 dB. At a normalised angular frequency $\Omega = \pi$, we compute the SVDs of $\hat{\boldsymbol{C}}(\mathrm{e}^{\mathrm{j}\pi})$ yielding singular values ς_m, $m = 1, 2$; their histograms are shown in Figs. 3(a) and (b). According to Fig. 2, we expect singular values of 0 and 1 for $\boldsymbol{A}(\mathrm{e}^{\mathrm{j}\pi})$, but ς_1 and ς_2 differ, and in particular the histogram for ς_1 in Fig. 3(a) does not include zero. △

The distribution for singular values (and likewise eigenvalues) are typically challenging to represent, but can be stated for specific cases, see e.g. [45]–[47]. For a complex Gaussian perturbation, a Rician fit for the histograms of Example 3 in Fig. 3 appears to be a close fit.

Since at a single frequency the probability of a zero singular value or of identical singular values is almost surely zero, this is also the case at any frequency. As a result, across the spectrum, the singular values of $\hat{\boldsymbol{C}}(\mathrm{e}^{\mathrm{j}\Omega})$ almost surely will not intersect or possess zero crossings.

Example 4: For one instance of a randomly perturbed $\hat{\boldsymbol{C}}(z)$ from Example 3, evaluating bin-wise SVDs with a sufficiently high spectral resolution of 2^{12} bins provides the evolution of singular values with frequency depicted in Fig. 4. The zoomed inserts of Fig. 4 demonstrate how singular values on the unit circle no longer intersect and also no longer possess zero crossings. △

Note that due to the loss of zero-crossings and intersections, the singular values of $\hat{\boldsymbol{C}}(z)$ are now 2π-periodic on the unit circle, and oversampling is no longer required. As the perturbation $\boldsymbol{E}(z)$ decreases, the analytic singular values of $\hat{\boldsymbol{C}}(z)$ converge towards functions that are piece-wise analytic segments of the analytic singular values of $\boldsymbol{C}(z)$, approximating non-differentiable functions at frequencies where previously intersections and zero-crossings occurred [44].

C. Perturbation of Singular Vectors

Sec. IV-B has outlined how perturbed singular values converge towards the piece-wise analytic SVD of $\boldsymbol{C}(z)$ as the perturbation decreases. The segments are switched where the analytic singular values of $\boldsymbol{C}(z)$ intersect. This also switches the corresponding analytic singular vectors; since singular vectors should be mutually orthogonal, for decreasing perturbations, the analytic singular vectors of $\hat{\boldsymbol{C}}(z)$ converge towards discontinuities at the switching frequencies. We demonstrate this by the following example.

Example 5: For the perturbed matrix of Example 4, we assess the subspace evolution of the left-singular vectors $\hat{\boldsymbol{u}}_m(z)$ with frequency. In order to ignore phase ambiguities across bins, we measure the Hermitian angle $\alpha_m(\Omega)$,

$$\cos\alpha_m(\Omega) = |\mathbf{r}^{\mathrm{H}}\boldsymbol{u}_m(\mathrm{e}^{\mathrm{j}\Omega})| \,, \tag{8}$$

against the reference vector $\mathbf{r} = \boldsymbol{u}_1(\mathrm{e}^{\mathrm{j}0})$. The resulting angles $\alpha_m(\Omega)$ are depicted in Fig. 5. Underlaid in grey are the angles for the unperturbed matrix $\boldsymbol{C}(z)$, while the subspace angles for $\hat{\boldsymbol{C}}(z)$ approximate discontinuities at the frequencies where the corresponding singular values in Fig. 4 are switched. △

D. Consequences for Precoding and Equalisation

Based on the findings above, a random perturbation ensures that an analytic SVD exists without the need for oversampling by $\kappa = 2$ in (1). As the perturbation term decreases, e.g. by performing system identification based on a large data set, the accuracy increases and $\hat{\boldsymbol{C}}(z)$ tends towards $\boldsymbol{C}(z)$, but the same cannot be said for the SVD factors. These tend towards piece-wise analytic functions, and the transition to (1) only occurs if the perturbation term is zero. In the transition, we find that the smaller the perturbation, the more difficult the approximation of a non-differentiability in terms of the singular values, and of a discontinuity in case of the singular vectors, becomes. Hence paradoxically, the more accurate $\hat{\boldsymbol{C}}(z)$ is, the

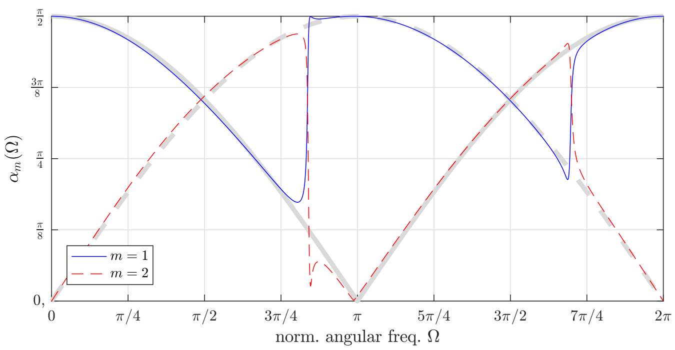

Fig. 5. Hermitian angles $\alpha_m(\Omega)$ according to (8) for the left-singular vectors of the perturbed matrix $\hat{\boldsymbol{C}}(z)$, with those for the unperturbed matrix $\boldsymbol{C}(z)$ underlaid in grey.

higher the approximation order grows that is required for an accurate representation of the singular vectors, and thus for the SVD-based precoding and equalisation operators in a MIMO communications system.

V. Recovering Ground Truth Singular Values

In order to estimate the ground truth analytic singular values of $\boldsymbol{C}(z)$ from a perturbed measurement $\hat{\boldsymbol{C}}(z)$, below we investigate an extension of a similar algorithm for the extraction of perturbed singular values in [38]. The algorithm is modified to address (i) singular values that can become negative, and (ii) singular values that may require a fractional delay in order to avoid oversampling by $\kappa = 2$ for an analytic solution [20], which is not required for the analytic eigenvalue decomposition [18], [19].

The approach is based on the fundamental property of analytic functions to match their Taylor series everywhere; as a result, the entire analytic function can be reconstructed from any small segment. Thus, we first identify segments of bin-wise singular values in Sec. V-A that can be clearly associated where a sufficient separation between singular values and zero-crossings exist. In order to align these segments, Sec. V-B compares their partial time-domain reconstructions, permitting the extraction of the ground truth singular values in Sec. V-C.

A. Segmentation

By operating in the discrete Fourier transform (DFT) domain, we perform a bin-wise SVD in each frequency bin of $\hat{\boldsymbol{C}}(\mathrm{e}^{\mathrm{j}\Omega_k})$, $\Omega_k = 2\pi k/K$, $k = 0, \dots, (K-1)$, where K is the DFT length, such that

$$\hat{\boldsymbol{C}}(\mathrm{e}^{\mathrm{j}\Omega_k}) = \mathbf{U}_k \boldsymbol{\Sigma}_k \mathbf{V}_k^{\mathrm{H}} \ , \qquad (9)$$

where $\boldsymbol{\Sigma}_k = \mathrm{diag}\{\sigma_{k,1}, \dots, \sigma_{k,M}\}$ with $\sigma_{k,1} \geq \dots \geq \sigma_{k,M} \geq 0$. In order to identify viable segments where singular values are sufficiently separated from each other and from any zero-crossings, we define a minimum distance as

$$d_{\min}(\Omega_k) = \min_{\substack{m,\mu=1,\dots,M \\ m\neq\mu}} \{(\sigma_{k,m} - \sigma_{k,\mu}), 2\sigma_{k,m}\} \ . \qquad (10)$$

The second argument in (10) measures the distance from a zero-crossing.

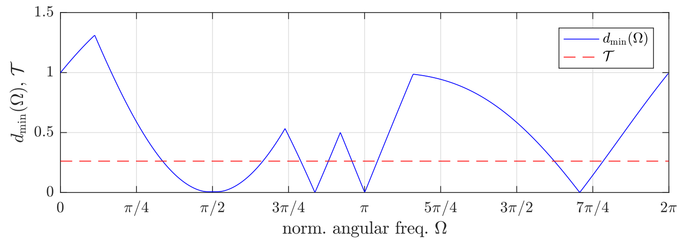

Fig. 6. Minimum distance of bin-wise singular values of $\hat{\boldsymbol{C}}(\mathrm{e}^{\mathrm{j}\Omega_k})$ of Example 6 compared to the threshold $\mathcal{T}$.

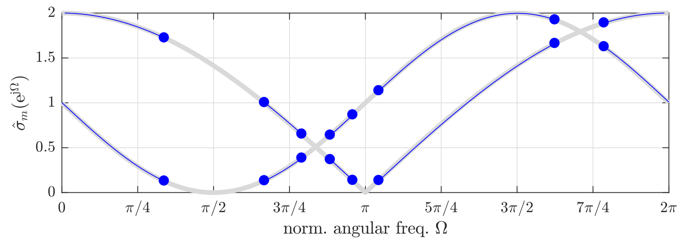

Fig. 7. Extracted $Q = 4$ segments for Example 6 based on the minimum distance and threshold in Fig. 6.

Segments can be defined where a sufficient number of subsequent frequency bins have a minimum distance above a preset threshold $\mathcal{T}$. For reasons of robustness, such segments must also satisfy a minimum length — i.e. a minimum number of consecutive frequency bins — in order to calculate a reliable reconstruction later [38].

Example 6: We now assume that $\boldsymbol{C}(z)$ is perturbed by a term $\boldsymbol{E}(z)$ at 60 dB SNR. The minimum distance $d_{\min}(\Omega_k)$ of bin-wise singular values in $K = 2^{10}$ DFT bins as defined in (10) is shown in Fig. 6. Valid segments are extracted where more than 16 successive bins satisfy a minimum distance $d_{\min}(\Omega_k) > \mathcal{T} := \frac{1}{5}\max_{\Omega_k}\{d_{\min}(\Omega_k)\}$. The resulting $Q = 4$ segments are shown in Fig. 7; note that the last segment wraps around at $\Omega = 2\pi$. △

B. Aligning Partial Reconstructions

Each segment can be converted back into the time domain using a partial inverse DFT [38]. We here apply a small modification, since segments potentially have to be fractionally delayed in case they belong to ground truth singular values with an odd number of zero crossings. Thus, we check if a phase shift equivalent to a half sample delay provides a symmetric response in the time domain. If this is the case, then for this particular singular value segment a fractional delay is incorporated.

Example 7: For the segments in Example 6, Fig. 8 shows the time domain reconstructions. Note that for each segment, one of the singular values has been corrected by a fractional delay of a half sample, resulting in functions that are symmetric w.r.t. $\tau = \frac{1}{2}$. Note that two of these fractionally delayed segments ($q = 3, 4$) exhibit a sign change. △

The alignment of the reconstructed segments uses the Hungarian algorithm [48], [49] based on the norm difference between different segments, taking into account that a smaller norm may be possible if a segment is negated. In Fig. 8, the

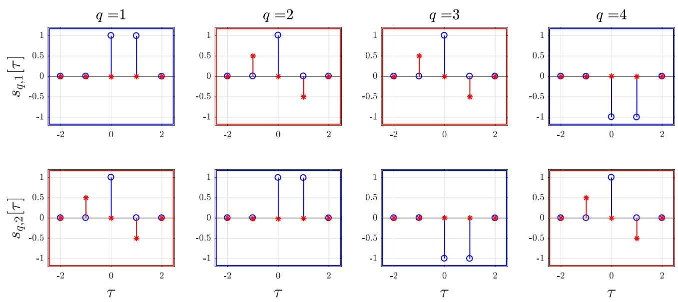

Fig. 8. Partial IDFT reconstructions of the segments in Fig. 7 with a potential half sample delay compensation in case the delayed version retains symmetry; real parts of $s_{q,m}[\tau]$ are shown as blue (∘), imaginary parts as red (∗) stems; frame colours of the subplots indicate their association.

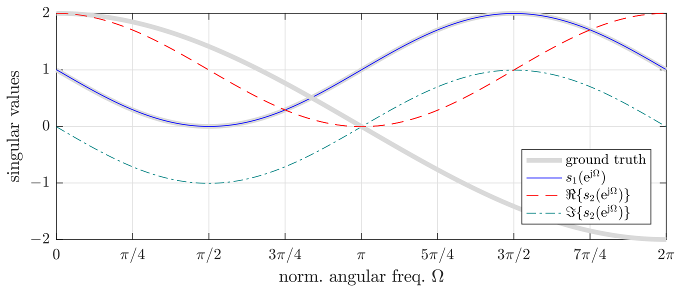

Fig. 9. Extracted singular values on the unit circle; to avoid oversampling, the real-valued constraint has been dropped [20].

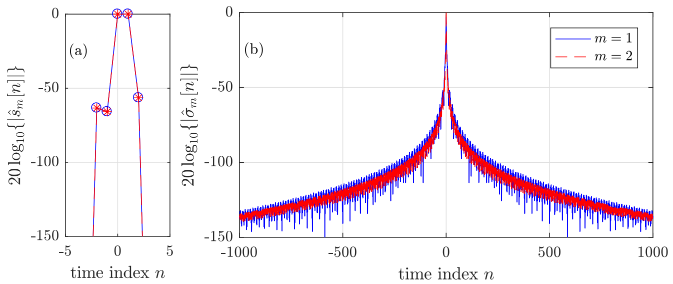

Fig. 10. Moduli of the time-domain singular values sw(a) obtained using (a) the proposed method and (b) an IDFT reconstruction based on the perturbed system in Fig. 4.

result of this alignment is indicated by the frame colours of the subplots.

C. Extraction of Analytic Singular Values

The extraction of singular values follows the procedure in [38], whereby a weighted average over the differently aligned and sign-corrected segments is performed. The weighting is provided by the length of the segments, whereby longer segments are deemed to be more reliable than shorter ones.

Example 8: For the segments in Example 7, Fig. 9 shows the segment-weighted and sign-corrected averages for the two singular vectors. In order to avoid oversampling by $\kappa = 2$, the half-sampled delay has now created a singular value $s_2(z)$ that is no longer constrained to be real-valued on the unit circle. Fig. 9 therefore contains the real- and imaginary parts of $s_2(e^{j\Omega})$, which now are 2π-periodic and therefore admit analyticity of $s_2(z)$. The support of the extracted singular values of 7 samples is close to the ground truth with a support of 3 coefficients.

For comparison, if instead of seeking the ground truth solution, we reconstruct the bin-wise SVDs of $\hat{\boldsymbol{C}}(z)$ as shown in Fig. 4, instead of a support of 7 as highlighted in Fig. 10(a), we end up with a support that is several orders of magnitude larger: Fig. 10(b) shows an IDFT with 2^{15} bins, where the decay of the coefficients is very slow. This represents the type of time-domain support that may be necessary, unaffected by any phase smoothing, if a bin-wise or per-subcarrier SVD is interpolated without addressing the challenges of the underlying analytic SVD.

VI. Conclusions

Motivated by the efforts in phase smoothing for precoding matrices in multicarrier MIMO communication systems, we have explored the analytic singular value decomposition as the theoretical foundation for the spectral coherence behind a per-subcarrier SVD. This reveals some of the challenges in trying to find a smooth interpolation from a limited number of subcarriers. Firstly, in order to admit the infinite differentiability and hence smoothness afforded by analytic functions, we have demonstrated the need for admitting complex valued singular values. Secondly, fundamental challenges arise from random perturbations introduced in the estimation process of the channel matrix. Paradoxically, the better the estimate, the higher may be the required approximation order of the singular values and their associated left- and right-singular vectors. Profoundly, this can lead to precoding and equalisation matrices being difficult to interpolate.

While we have not yet addressed the recovery of analytic singular vectors, we have as a first step demonstrated how to extract analytic singular values by adapting an existing approach for analytic eigenvalues from [38]. Despite the above problems, this can recover smooth solutions with compact support, that hence are easier to interpolate. For the somewhat analogous case of an analytic eigenvalue decomposition, once analytic eigenvalues have been extracted [50]–[52], their corresponding eigenvectors can be tackled [53], [54].

References

[1] G. W. Stewart, "On the early history of the singular value decomposition," *SIAM Review*, vol. 35, no. 4, pp. 551–566, 1993.

[2] G. H. Golub and C. F. Van Loan, *Matrix Computations*, 3rd ed. Baltimore, Maryland: John Hopkins University Press, 1996.

[3] D. Palomar, J. Cioffi, and M. Lagunas, "Joint Tx-Rx beamforming design for multicarrier MIMO channels: a unified framework for convex optimization," *IEEE Trans. Signal Process.*, vol. 51, no. 9, pp. 2381–2401, 2003.

[4] M. Vu and A. Paulraj, "MIMO Wireless Linear Precoding," *IEEE Signal Process. Mag.*, vol. 24, no. 5, pp. 86–105, Sep. 2007.

[5] V. Neo, S. Redif, J. McWhirter, J. Pestana, I. Proudler, S. Weiss, and P. Naylor, "Polynomial eigenvalue decomposition for multichannel broadband signal processing," *IEEE Signal Process. Mag.*, vol. 40, no. 7, pp. 18–37, Nov. 2023.

[6] L. Hanzo, Y. Akhtman, L. Wang, and M. Jiang, *MIMO-OFDM for LTE, Wi-Fi and WiMAX*. John Wiley & Sons, 2010.

[7] R. Marsalek, J. Blumenstein, J. Vychodil, T. Mikulasek, P. Jung, and A. Pfadler, "Real-world OTFS channel estimation performance evaluation on mmwave vehicular channels," in *27th Workshop on Smart Antennas*, Dresden, Germany, 2024, pp. 1–7.

[8] P. Hoeher, S. Kaiser, and P. Robertson, "Two-dimensional pilot-symbol-aided channel estimation by Wiener filtering," in *IEEE Int. Conf. Acoustics, Speech, and Signal Process.*, vol. 3, Munich, Germany, Apr. 1997, pp. 1845–1848 vol.3.

[9] Y. Li, "Simplified channel estimation for OFDM systems with multiple transmit antennas," *IEEE Trans. Wireless Comm.*, vol. 1, no. 1, pp. 67–75, 2002.

[10] C. Shen and M. P. Fitz, "MIMO-OFDM beamforming for improved channel estimation," *IEEE J. Sel. Areas Comm.*, vol. 26, no. 6, pp. 948–959, 2008.

[11] J. Choi and R. Heath, "Interpolation based transmit beamforming for MIMO-OFDM with limited feedback," *IEEE Trans. Signal Process.*, vol. 53, no. 11, pp. 4125–4135, 2005.

[12] W. Hu, F. Li, and Y. Jiang, "Phase rotations of SVD-based precoders in MIMO-OFDM for improved channel estimation," *IEEE Wireless Comm. Lett.*, vol. 10, no. 8, pp. 1805–1809, 2021.

[13] K. Schober, R. Wichman, and M. Enescu, "Geodesical refinement of MIMO limited feedback," *IEEE Trans. Comm.*, vol. 64, no. 3, pp. 1031–1041, 2016.

[14] J. Liu, W. Zhang, and Y. Jiang, "Channel estimation considerate precoder design for multi-user massive MIMO-OFDM systems: The concept and fast algorithms," *IEEE Trans. Comm.*, vol. 73, no. 6, pp. 3820 - 3832, Jun. 2025.

[15] A. Pfadler, T. Szollmann, P. Jung, and S. Stańczak, "Estimation of doubly-dispersive channels in linearly precoded multicarrier systems using smoothness regularization," *IEEE Trans. Wireless Comm.*, vol. 23, no. 2, pp. 1293–1307, 2024.

[16] J. G. McWhirter, P. D. Baxter, T. Cooper, S. Redif, and J. Foster, "An EVD Algorithm for Para-Hermitian Polynomial Matrices," *IEEE Trans. Signal Process.*, vol. 55, no. 5, pp. 2158–2169, May 2007.

[17] I. Gohberg, P. Lancaster, and L. Rodman, *Matrix Polynomials*. SIAM, 2009.

[18] G. Barbarino and V. Noferini, "On the Rellich eigendecomposition of para-Hermitian matrices and the sign characteristics of $*$-palindromic matrix polynomials," *Linear Algebra Appl.*, vol. 672, pp. 1–27, Sep. 2023.

[19] S. Weiss, I. K. Proudler, G. Barbarino, J. Pestana, and J. G. McWhirter, "On properties and structure of the analytic singular value decomposition," *IEEE Trans. Signal Process.*, vol. 72, pp. 2260–2275, 2024.

[20] G. Barbarino, "On the periodicity of singular vectors and the holomorphic block-circulant SVD on the unit circumference," *Linear Algebra Appl.*, vol. 721, pp. 465–483, Sep. 2025.

[21] P.P. Vaidyanathan, *Multirate Systems and Filter Banks*. Englewood Cliffs: Prentice Hall, 1993.

[22] B. De Moor and S. Boyd, "Analytic properties of singular values and vectors," KU Leuven, Tech. Rep., 1989.

[23] A. Bunse-Gerstner, R. Byers, V. Mehrmann, and N. K. Nicols, "Numerical computation of an analytic singular value decomposition of a matrix valued function," *Numer. Math*, vol. 60, pp. 1–40, 1991.

[24] Y.-F. Chou and T.-H. Sang, "Efficient interpolation of precoding matrices in MIMO-OFDM systems," in *IEEE 11th Workshop Signal Process. Adv. Wireless Comm.*, Marrakech, Morocco, Jun. 2010, pp. 1–4.

[25] P. Mehta, A. S. Bharath, K. Appaiah, R. Velmurugan, and D. Pal, "Lattice all-pass filter based precoder adaptation for MIMO wireless channels," *IEEE Trans. Vehic. Techn.*, vol. 73, no. 11, pp. 16905-16916, 2024.

[26] S. Weiss and M. D. Macleod, "Maximally smooth Dirichlet interpolation from complete and incomplete sample points on the unit circle," in *IEEE Int. Conf. Acoustics, Speech, and Signal Process.*, Brighton, UK, May 2019.

[27] S. Weiss, J. Selva, and M. D. Macleod, "Measuring smoothness of trigonometric interpolation through incomplete sample points," in *28th European Signal Process. Conf.*, Amsterdam, Netherlands, Jan. 2021, pp. 2319–2323.

[28] M. A. Bakhit, F. A. Khattak, I. K. Proudler, S. Weiss, and G. W. Rice, "Compact order polynomial singular value decomposition of a matrix of analytic functions," in *9th IEEE Workshop Comp. Adv. Multisensor and Array Processing*, Los Sueños, Costa Rica, Dec. 2023.

[29] M. A. Bakhit, F. A. Khattak, G. W. Rice, I. K. Proudler, and S. Weiss, "Recovering ground truth singular values from randomly perturbed MIMO transfer functions," in *23rd IEEE Statistical Signal Processing Workshop*, Edinburgh, Scotland, pp. 465–483, Jun. 2025.

[30] S. Weiss, S.J. Schlecht, and M. Moonen. "Polynomial Procrustes method for randomly perturbed near-paraunitary systems," in *23rd IEEE Statistical Signal Processing Workshop*, Edinburgh, Scotland, pp. 231-235, Jun. 2025.

[31] S. Weiss, S. J. Schlecht, and M. Moonen, "Best least squares paraunitary approximation: Analytic procrustes problem," *IEEE Trans. Signal Process.*, 2025, submitted.

[32] S. Nijhawan, A. Gupta, K. Appaiah, R. Vaze, and N. Karamchandani, "Flag manifold-based precoder interpolation techniques for MIMO-OFDM systems," *IEEE Trans. Comm.*, vol. 69, no. 7, pp. 4347–4359, 2021.

[33] C. H. Ta and S. Weiss, "A design of precoding and equalisation for broadband MIMO systems," in *41st Asilomar Conf. Signals, Systems and Computers*, Pacific Grove, CA, USA, Nov. 2007, pp. 1616–1620.

[34] N. Moret, A. Tonello, and S. Weiss, "MIMO precoding for filter bank modulation systems based on PSVD," in *IEEE 73rd Vehic. Tech. Conf.*, May 2011, pp. 1–5.

[35] S. Weiss, N. Moret, A. Millar, A. Tonello, and R. Stewart, "Initial results on an MMSE precoding and equalisation approach to MIMO PLC channels," in *IEEE Int. Symp. Power Line Communications and Its Appl.*, Apr. 2011, pp. 146–152.

[36] X. Mestre and D. Gregoratti, "A parallel processing approach to filterbank multicarrier MIMO transmission under strong frequency selectivity," in *IEEE Int. Conf. Acoustics, Speech and Signal Process.*, May 2014, pp. 8078–8082.

[37] S. Weiss and G. Barbarino, "Relations between analytic spectral and singular value decompositions," in *33rd European Signal Process. Conf.*, Isola delle Femmine, Italy, Sep. 2025.

[38] S. J. Schlecht and S. Weiss, "Reconstructing analytic dinosaurs: Polynomial eigenvalue decomposition for eigenvalues with unmajorised ground truth," in *32nd European Signal Process. Conf.*, Lyon, France, Aug. 2024, pp. 1287–1291.

[39] B. Widrow and S. D. Stearns, *Adaptive Signal Processing*. Englewood Cliffs, New York: Prentice Hall, 1985.

[40] S. Haykin, *Adaptive Filter Theory*, 2nd ed. Englewood Cliffs: Prentice Hall, 1991.

[41] C. Delaosa, J. Pestana, N.J. Goddard, S. Somasundaram, and S. Weiss: "Sample space-time covariance matrix estimation," in *IEEE Int. Conf. Acoustics, Speech, and Signal Process.*, Brighton, UK, pp. 8033-8037, May 2019.

[42] C. Delaosa, J. Pestana, I. K. Proudler, and S. Weiss, "Impact of space-time covariance matrix estimation on bin-wise eigenvalue and eigenspace perturbations," *Signal Process.*, vol. 233, p. 109946, Aug. 2025.

[43] G. Stewart, "Perturbation theory for the singular value decomposition," Institute for Advanced Computer Studies, Univ. of Maryland, Tech. Rep. UMIACS-TR-90-124, Oct. 1990.

[44] M. Bakhit, F. A. Khattak, I. K. Proudler, and S. Weiss, "Impact of estimation errors of a matrix of transfer functions onto its analytic singular values and their potential algorithmic extraction," in *IEEE High Performance Extreme Computing Conf.*. Boston, MA, Sep. 2024, pp. 1–7.

[45] J.-M. Azaïs and M. Wschebor, "Upper and lower bounds for the tails of the distribution of the condition number of a gaussian matrix," *SIAM J. Matrix Analysis & Appl.*, vol. 26, no. 2, pp. 426–440, 2004.

[46] T. Ratnarajah, R. Vaillancourt, and M. Alvo, "Eigenvalues and condition numbers of complex random matrices," *SIAM J. Matrix Analysis & Appl.*, vol. 26, no. 2, pp. 441–456, 2004.

[47] W. Anderson and M. T. Wells, "The exact distribution of the condition number of a gaussian matrix," *SIAM J.Matrix Analysis & Appl.*, vol. 31, no. 3, pp. 1125–1130, 2010.

[48] H. W. Kuhn, "The Hungarian method for the assignment problem," *Naval Research Logistics Quarterly*, vol. 2, no. 1-2, pp. 83–97, 1955.

[49] J. Munkres, "Algorithms for the assignment and transportation problems," *Journal of the Society for Industrial and Applied Mathematics*, vol. 5, no. 1, pp. 32–38, 1957.

[50] S. Weiss, I.K. Proudler, F.K. Coutts, and J. Pestana, "Iterative approximation of analytic eigenvalues of a parahermitian matrix EVD," in *IEEE Int. Conf. Acoustics, Speech and Signal Process.*, Brighton, UK, May 2019.

[51] S. Weiss, I.K. Proudler, and F.K. Coutts, "Eigenvalue decomposition of a parahermitian matrix: extraction of analytic eigenvalues," *IEEE Trans. Signal Process.*, vol. 69, pp. 722–737, Jan. 2021.

[52] F.A. Khattak, I.K. Proudler, and S. Weiss, "Scalable analytic eigenvalue extraction algorithm," *IEEE Access*, vol. 12, pp. 166 652–166 659, Dec. 2024.

[53] S. Weiss, I.K. Proudler, F.K. Coutts, and J. Deeks, "Extraction of analytic eigenvectors from a parahermitian matrix," in *Int. Conf. Sensor Signal Processing or Defence*, Edinburgh, UK, 2020.

[54] S. Weiss, I.K. Proudler, F.K. Coutts, and F.A. Khattak, "Eigenvalue decomposition of a parahermitian matrix: extraction of analytic eigenvectors," *IEEE Trans. Signal Process.*, vol. 71, pp. 1642–1656, Apr. 2023.